Photochemistry of XCH2CN (X = -Cl, -SH) in Argon Matrices

Joanna Zapala, Thomas Custer, Jean-Claude Guillemin, Marcin Gronowski

Photochemistry of XCH_2CN (X=-Cl,-SH) in Argon Matrices

Joanna Zapała [a], Thomas Custer [a], Jean-Claude Guillemin [b], Marcin Gronowski [a]

[a] Institute of Physical Chemistry, Polish Academy of Sciences, Kasprzaka 44/52, PL-01-224 Warsaw, Poland

[b] Univ Rennes, Ecole Nationale Supérieure de Chimie de Rennes, CNRS, ISCR – UMR6226, F-35000 Rennes, France.

*E-mail jzapala@ichf.edu.pl

Abstract

We report infrared spectra and photochemical behavior of the potentially astrochemically significant species, mercaptoacetonitrile ($HS\text{-}CH_2C{\equiv}N$) and, for comparison purposes, chloroacetonitrile ($Cl\text{-}CH_2C{\equiv}N$), both suspended in an argon matrix at 6K. Photolytic formation of the isocyano products $HS\text{-}CH_2\text{-}NC$ and $Cl\text{-}CH_2\text{-}NC$ were observed as well as CH_3NSC and CH_3SCN (in $HS\text{-}CH_2CN$ photolysis). While no dissociation products were observed for $Cl\text{-}CH_2\text{-}CN$, photolysis of $HS\text{-}CH_2\text{-}CN$ produced compounds necessitating the loss of the CN group to form $CH_2{=}S$, the SH group to form $H_2C\text{-}CN$ and HC-CN, or both CN and SH to form CH_3 and CH_4. Observation of emission spectra upon annealing indicates the presence of free sulfur atom in matrices of photolyzed $HS\text{-}CH_2\text{-}CN$.

1. Introduction

Theoretical studies[1] show that mercaptoacetonitrile ($HS\text{-}CH_2\text{-}CN$), methyl isothiocyanate (CH_3NCS), and methyl thiocyanate (CH_3SCN) are the three most stable molecules of the C_2H_3NS family having energies of 0, 7.8, and 12.4 kJ/mol respectively. Although not yet detected in the interstellar medium (ISM), each of these can be

considered as a potential candidate. The structurally similar species CH_3SH[2], HSCN[3,4], HNCS[3,4], and CH_3CN[5,6] have all been detected in the ISM. Hydroxyacetonitrile (HO-CH_2-CN), the closest oxygen-bearing analogue of mercaptoacetonitrile, has been observed in laboratory generated interstellar and cometary ice analogs[7] and recently detected in solar-type protostar IRAS16293–2422 B[8]. It is not difficult to imagine replacement of an H atom with a CN, NC, or SH group, or addition of a CH_2 or S to one of these known astrochemical species to reach the lowest energy members of the C_2H_3NS chemical family.

While structural analogies are interesting, explicit pathways for formation or decomposition of S containing species in space, whether they have already been detected or are promising candidates, should be elucidated in the laboratory and through calculations. Existing models and the ratio of abundances of different sulfur species have already been used to evaluate the age of interstellar clouds[9,10,11] and to estimate the mass of an emerging star[12]. However, problems encountered in determination of sulfur abundance in the interstellar medium[13], describing the interstellar synthesis of methanethiol (detected in Sagittarius B2 core[14] and hot core of G327.3-0.6[15] but absent in TMC-1), and prediction of abundances of nearly all sulfur-containing molecules detected in TMC-1[16,17,9] suggest that our current understanding of sulfur chemistry remains incomplete.

Here we explore one aspect of sulfur chemistry by describing the computational and experimental results of the UV photolysis of mercaptoacetonitrile (HS-CH_2-CN, MAN) and its closely related synthetic precursor chloroacetonitrile (Cl-CH_2-CN, CAN) in noble gas matrices. Although CAN is not of obvious astrochemical significance (Cl abundance

is generally not high in the universe and only a handful of species including AlCl, KCl, NaCl, HCl, HCl^+, H_2Cl^+, and CH_3Cl[18] have so far been detected), no noble gas matrix photolysis experiments have been performed on this species. As detailed spectroscopic information for this molecule is available, photolysis of this chemical provides a convenient comparison with mercaptoacetonitrile. While chemically inert noble gas matrices are not considered good models for authentic interstellar ices[19], photochemistry measurements in this environment can be treated as a first, necessary step toward understanding the transformations that might result in a more representative but chemically complex ice environment. They also provide a means to produce more exotic isomers for spectroscopic characterization. Photochemistry in pertinent interstellar ice analogues (e.g., containing CO, H_2O, or other species or mixtures [20]) is the next step along the path towards understanding photochemical processing in space and will be the subject of a future publication.

Of the three lowest energy C_2H_3SN family members, mercaptoacetonitrile (HS-CH_2-CN), which has a weak chemical stability at room temperature, is the only one not commercially available and is therefore less well studied. Nevertheless, this species has been explicitly discussed as a likely astrochemical species whose potential routes of formation in the interstellar medium were explored and microwave spectrum experimentally measured at both -30 °C and room temperature[21]. Synclinal and anti-periplanar conformers of mercaptoacetonitrile were identified and their energetic separation measured to be 3.8±0.3 kJ/mol. A theoretical study of these two conformers has also recently been made in an effort to understand their potential behavior in harsh astrophysical environments[22]. The charge transfer dynamics resulting from collisions

between energetic protons and these isomers was explored and compared to the two lowest-energy HCN dimers (Z and E isomers of cyanomethanimine). Charge transfer of the synclinal conformer turned out to be more efficient than for the corresponding cyanomethanimine.

Outside of these recent works, only a handful of studies on mercaptoacetonitrile are available in the literature. Several synthetic routes to its formation have been explored and routine ^{1}H and ^{13}C NMR as well as mass spectrometry and IR spectroscopy were used to characterize the products[23,24,25,26]. Most pertinent to the work at hand are spectroscopic measurements in the infrared and all reported spectra to date are for the pure liquid. Early work of Mathais et al.[23] reported six vibrational bands: the SH group at 2560 and 920 cm^{-1}; the CN group at 2240 cm^{-1}; and the CH_2 group at 2980, 2940 and 1400 cm^{-1}. Wepplo [24] gave five unassigned vibrations: 2680, 2260, 990, 925 and 710 cm^{-1}.Gaumont et al.[25] reported the SH vibration at 2560 cm^{-1} and CN vibration at 2220 cm^{-1}. Finally, Alexander et al.[26] reported a CN vibration at 2247cm^{-1}. Aside from the vibration at 2680 cm^{-1}[24], possibly meant to be 2980 cm^{-1}, these comprise a consistent summary of vibrations for this molecule in the liquid phase. They are collected and presented with our results in **Table1 Supporting Information**. No more detailed IR spectral data of mercaptoacetonitrille is available.

As for the commercially available chloroacetonitrile (Cl-CH_2-CN), numerous publications are available and include measurements using a variety of spectroscopic methods. Infrared data was first available in the 1950's, when Zeil et al.[27] performed measurements of pure Cl-CH_2-CN using IR and Raman spectroscopy and gave a comprehensive list of fundamental vibrations as well as some of their combinations.

Since 50's, various other groups have performed measurements in the gas-phase [28, 29] or in the liquid-phase [30, 29]. Researchers have described the effects of solvation [31], [28, 32], complexation [33], or change of chlorine substituent [34] on the position of various bands. IR band positions [35] and intensities [36] have also been calculated. Nemes et al.[37] estimated absolute intensities for eight vibrations found in the liquid phase and, later the same year [38], refined the position of the vibrations and compared their intensities with what was measured in the gas phase as well as in carbon disulfide (CS_2). Thomas et al.[39] investigated the CN stretching band in more detail and estimated its absolute intensity, focusing on the effect of environment and phase change on its intensity. Finally, George et al.[40] reported hydrogen chloride mode of Cl-CH_2-CN:HCl complex at 2709 cm^{-1} in an Ar matrix at 7K although no band positions for the matrix isolated Cl-CH_2-CN species alone were given. The positions and intensities of Cl-CH_2-CN vibrations published by abovementioned authors are collected in **Table2 Supporting Information**.

While the photochemistry of both HS-CH_2-CN and Cl-CH_2-CN species has not been described, a rich literature concerning transformations of small molecules is available to suggest potential processes that might occur upon UV irradiation. Due to the matrix cage effect [41, 42] loss of larger moities (e.g., fragments such as CN or CH_3) following bond breakage is generally not observed and isomerization is the most probable process. Nevertheless some fraction of these fragments may escape. Depending on the energy available and rare gas used, H, Cl or S atoms can end up being separated to leave radicals, ions, or other isomeric combinations.

Concerning isomerization of cyano species, UV irradiation of cyanoacetylene (HC_3N) trapped in noble gas matrix leads to the formation of several isomers of the parent

molecule, including isocyanoacetylene (HCCNC) and an imine (HNC_3)[43]. Both of these isomers have been already detected in the interstellar medium accompanying the more abundant cyanoacetylene. Kawaguchi et al. identified HCCNC[44] and later the same year HNCCC[45] in Taurus Molecular Cloud 1 (TMC-1). Gensheimer et al.[46] identified both isomers in IRC +10216 and Vastel et al. in the L1544 pre-stellar core[47]. The formation of isocyanides from cyano precursors in a matrix environment has been observed for a variety of unsaturated cyanoacetylenes including HC_3N, HC_5N[48], NC_4N [49], NC_6N[50], and C_2H_3CN[51] among others. Nevertheless, it is not a foregone conclusion that such cyano/isocyano rearrangement must occur for any arbitrary cyanide containing species.

Photolysis of thiol species of the form R-SH results mainly in scission of C-S and S-H bonds[52,53,54] with the main products being radicals and, depending on photolysis conditions, various radical recombination products. In 195 nm flash photolysis experiments on gaseous CH_3SH Callear et al. [52] observed formation of CH_3S, CH_3 and other radicals using UV absorption spectroscopy while 254nm photolysis of C_2H_5SH in a xenon matrix was shown to produce the thiyl radical $C_2H_5S^*$ [55]. Photolysis of CH_3SH vapor in 254 and 214 nm has been shown to produce H_2, H_2S, C_2H_4, C_2H_6 and CH_3SSCH_3[53]; C_2H_5SH vapor photolysed in the same conditions produced H_2, H_2S, C_2H_4, C_2H_6 [56] and $C_2H_5SSC_2H_5$[57].

Hydrogen atom production and escape of H_2 from the matrix cage has been reported as well, producing even more complex, dehydrogenated species, where photolysis of methanethiol at 121nm in a nitrogen matrix at 14 K leads to formation of CH_4, CS, CS_2, CH_3 and H_2CS as the main products[58].

Lastly, studies of photolysis of alkyl halides in matrixes[59, 60] show that the cage

effect can inhibit halogen detachment processes. Photolysis of methyl chloride CH_3Cl in Ar and N_2 matrixes[60] was found to yield CCl, HCCl and H_2CCl as major products in addition to smaller amounts of CH_3, HCl and CH_4.

Based on these works, the most likely result of mercaptoacetonitrile or chloroacetonitrile photolysis should involve CN/NC isomerization or be products of –H or –SH elimination.

2. Theoretical methods

A combination of two methods of solving the electronic Schrödinger equation was used for these studies to arrive at vibrational frequencies. Density functional theory with the 3-term correlation functional of Becke[61] and the exchange functional of Lee, Yang, and Parr[62] (B3LYP) were used with vibrational second-order perturbation theory[63,64,65,66] to calculate anharmonic frequencies and intensities. The *ab initio* coupled cluster method, truncated to iterative treatment of single and double excitations and the perturbative treatment of triple excitations (CCSD(T))[66,67,68,69,70,71] were used during computation of harmonic frequencies. The triple-ζ Dunning-type basis set (cc-pVTZ)[72] was chosen for the CCSD(T) calculations while its augmented version (aug-cc-pVTZ)[73] was used for B3LYP computations. All vibrational calculations were preceded by geometry optimization at the same level of electronic structure theory and the Gaussian 09[74] program was used for all computations.Vibrational frequencies ultimately reported were calculated using the following equation:

$$\nu_{rec} = \omega_{CCSD(T)} + (\nu_{B3LYP} - \omega_{B3LYP}); \quad (1)$$

where $\omega_{CCSD(T)}$ and ω_{B3LYP} are harmonic frequencies computed either using CCSD(T) or B3LYP methods and ν_{B3LYP} is the anharmonic frequency computed using B3LYP as described previously. This methodology has been successfully applied in earlier studies [75-77] and in other systems where the resulting vibrational frequencies generally had an accuracy better than 10 cm^{-1} [78].

3. Experimental methods

The HS-CH_2-CN used in these experiments was synthesized according to Gaumont et al.[25], purified as reported by Møllendal et al.[21] and stored either with or without Amberlyst at -80°C. This malodorous compound decomposes vigorously at room temperature or under basic conditions. The kinetic stability of this compound is strongly dependent on the temperature and the presence of acidic compounds. Although Amberlyst may stabilize the chemical for long-term storage, it also proved to be a strong source of methanol which was trapped in its pore spaces during previous synthetic steps. The chemical proved to be sufficiently stable without Amberlyst for use in these photolysis experiments.

Chloroacetonitrile, Cl-CH_2-CN was purchased (98%, abcr GmBH).

Spectroscopic measurements were performed on a Bruker Vertex 70 instrument equipped with a KBr beam splitter and liquid-nitrogen-cooled MCT (HgCdTe) detector in the 400-6000 cm^{-1} spectral range at the maximum available resolution of 0.16 cm^{-1}. Degassed HS-CH_2-CN or Cl-CH_2-CN was combined with Ar (5.0 Multax s.c.) at a ratio of 1:1000 in a stainless steel vacuum manifold with partial pressures measured using

capacitance manometers (10 torr and 1000 torr, MKS instruments). Following two hours to allow for mixing of HS-CH_2-CN or Cl-CH_2-CN with Ar in the manifold, samples were deposited onto a CsI window pre-cooled to 5-6 K inside a vacuum chamber (~10^{-7} Torr). Cooling was accomplished using a closed-cycle helium refrigerator (DE-202SE Advanced Research Systems) whose temperature was controlled using a LakeShore 325 temperature controller. The cold window was positioned at 45° with respect to the path of IR radiation of the spectrometer and deposition was carried out at a flow rate of ca. 0.1 mmol/minute through a capillary nozzle of 1 mm diameter terminating ~2cm from the cold window. The total amount of the mixture deposited never exceeded 8 mmol (~300 Torr).

Lower limits of absolute intensities were calculated using the formula from [79], by Szczepaniak et al.: $A\left[\frac{km}{mole}\right] = \frac{2.3031}{100 * c * D}\int log\frac{I_0}{I}dv$. In this expression, c is the molar concentration of HS-CH_2-CN or Cl-CH_2-CN in $\left[\frac{mmole}{cm^3}\right]$, D is the film thickness $[cm]$, $log\frac{I_0}{I}$ is the measured absorbance of the band, and ν is the wavenumber [cm^{-1}]. The molar concentration was calculated using $c = \frac{p(\mathrm{HSCH2CN\ or\ ClCH2CN})}{p(\mathrm{argon})} \cdot \rho$ where ρ is the density of solid argon with a value of 44 $\frac{mmole}{cm^3}$ [79] and p is the measured partial pressure of the pertinent species. It is assumed that both the chemical and the rare gas are sufficiently pure that the partial pressures measured are not affected by any other species and that this ratio is conserved through deposition and in the ice itself. Observed bands were integrated using the OPUS program (Bruker Optik GmbH 2014). The thicknesses of the deposited matrices were determined by monitoring reflected He-Ne laser light[80] as well as using interference fringes observable in IR spectra. For the laser thickness measurements, a fixed-frequency He-Ne laser (ThorLabs HNL050R model, λ = 632.5 nm) was directed

towards a growing matrix. Interference was produced in the laser light reflected by the vacuum-ice and ice-substrate interfaces which have different and changing optical paths as film growth proceeds. Reflected light intensity as a function of time was recorded using a portable CCD spectrometer equipped with a fiber optic that could be adjusted outside of the vacuum chamber to capture the reflected laser light (Mightex CCD, HRS series). The intensity of the reflected laser light oscillates between periods of constructive and destructive interference as a function of time. While the time of one oscillatory period is a function of deposition rate, the change in thickness produced over the course of one period is constant. Because of this, the total thickness of a matrix can be estimated by counting the number of fringes starting from time zero until deposition is stopped (or an arbitrary time of interest) and using the following relationship presented by Urso et al.[80]: $D = m\Delta d = \frac{m\lambda_0}{2n_f\sqrt{1-sin^2\theta_i/n_f^2}}$. In this equation, D is the film thickness (total thickness of the matrix) [cm], m is the number of fringes observed, Δd is the thickness increase between two fringes [cm], θ_i is incidence angle of the laser with respect to the cold target, n_f is the refractive index of the film, and λ_0 is the wavelength of laser light: 6.325x10^{-5} [cm]. We assumed n_f to be similar to pure argon for our experimental conditions, a reasonable assumption given the 1:1000 ratio of chemical to Ar. A refractive index value of 1.52 was used for solid Ar at 6 K[81]. Thickness information can also be retrieved from IR spectra directly using interference fringes which, in a well ordered ice, manifest as an undulating baseline in our spectra. In this method, a modified equation was used [80]: $D = \frac{1}{l * 2n_f\sqrt{1-\frac{sin^2\theta_i}{n_f^2}}}$, where D is the film thickness [cm], l is the distance between the fringes [cm^{-1}], θ_i is incidence angle of the IR light with respect to the cold target, and n_f is the refractive index

of the film. The equivalence of these two methods of thickness determination was verified for pure Ar matrices by depositing a measured amount of noble gas while monitoring using laser interference fringes. At specified points, deposition was interrupted (0.625 mmol, 1.25 mmol, 2.5 mmol, 3.75 mmol, and 5 mmol) so IR spectral fringes could be measured. Good agreement between both methods was obtained with a difference of approximately 10%. In another series of experiments, thickness estimated from the pattern in our IR spectra was measured as a function of incident angle θ_i and gave an error typically less than 2%.

Both HS-CH_2-CN and Cl-CH_2-CN were exposed to UV irradiation generated by an excimer laser. HS-CH_2-CN samples were irradiated either using at 248 nm (KrF excimer) for 2.5 hours or 193 nm (ArF excimer) for 1.5-2.5 hours with an average laser pulse frequency of 10 Hz and power of 1 mJ per pulse (approx. 0.2 mJ/cm^3) measured just in front of the quartz window of the vacuum chamber using a pyroelectric sensor (Ophir Optronics PE50B). Cl-CH_2-CN was irradiated at 193 nm (ArF excimer) for 2 hours with an average laser pulse frequency of 10 Hz and power of 0.5 mJ per pulse (approx. 0.1 mJ/cm^3). Annealing was performed as the last step of sample processing and consisted of raising the temperature of the sample to ~35 K for a period of 20 min and then re-cooling to the original value. Emission observed during annealing was recorded using a Mightex CCD spectrometer (HRS series, 300-1070 nm spectral range, 1.7 nm resolution). IR spectra taken following annealing were used to confirm that various groups of product signals belonged to the same species (either increasing or decreasing together).

4. Results

4.1 Theory

Theoretical IR frequencies, intensities, and rotational constants for mercaptoacetonitrile (HS-CH_2-CN) along with other C_2H_3SN isomers have been published previously[1]. Only a comparison of predicted anharmonic IR frequencies for synclinal and anti-periplanar conformers, not provided in the previous work, are given here in **Table 1**. Similar calculations to those performed for C_2H_3SN isomers were also performed for the C_2H_2NCl family of isomers which includes Cl-CH_2-CN (CAN). First, B3LYP/aug-cc-pVTZ computations were used to estimate relative energies for different isomers of the C_2H_2NCl family (**Fig 1**) starting from structures for which Lewis dot diagrams could be drawn as closed shell molecules. Both singlet and triplet states were optimized for each structure. More precise computations at the CCSD(T)/cc-pVTZ level were then performed for CAN, CAN-1, and CAN-2. The relative energies are collated in **Fig 1** and vibrational frequencies in **Tables 2A**, **2B**, and **2C**. Although CAN isomers are not likely candidates for detection in space, the microwave spectrum of CAN has already been reported and the rotational constants and dipole moments for the three lowest energy isomers of CAN given in **Table 3** may prove useful for an eventual radioastronomical search or microwave measurements**.** In this table, ground state rotational constants are calculated at the CCSD(T)/cc-pVTZ level of theory and differences between ground state and equilibrium rotational constants at B3LYP/aug-cc-pVTZ. Without including core electron correlation and approaching the complete basis set limit, the precision of these rotational constants is likely a little more than 1%, a limitation that will be addressed in a future publication.

The predicted dipole moments for these molecules are high, which suggests that their detection during any eventual experimental rotational spectroscopy studies should be facile.

Fig 1 Structures of isomers of C_2H_2ClN stoichiometry. The B3LYP relative energies are given for all isomers, while CCSD(T) (bold in parenthesis) relative energies are given only for the three lowest energy isomers.

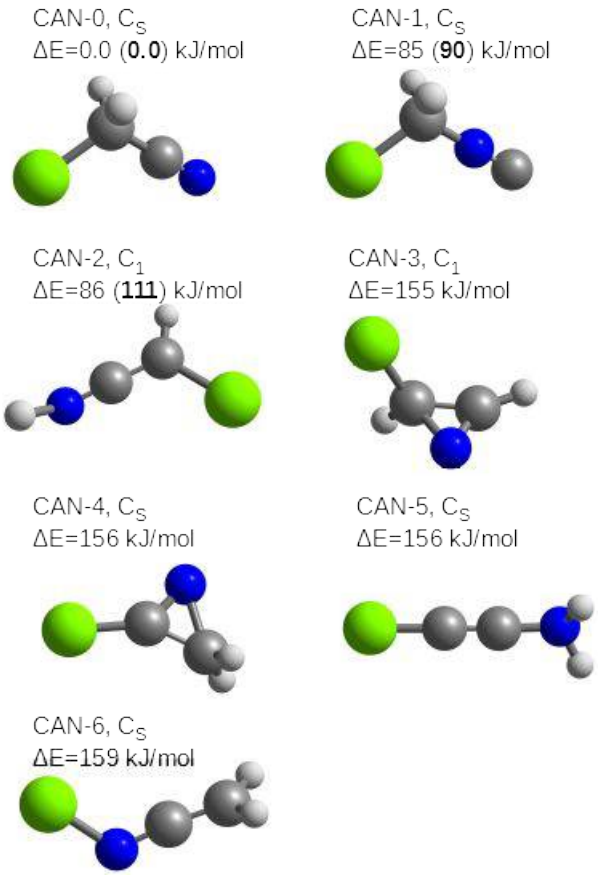

Table 1 Comparison of predicted frequencies and intensities for two conformers of HS-CH_2-CN (MAN) along with experimental values measured in an Ar matrix.

Mode [g]	Freq. [cm^{-1}]			Inten. [km mol^{-1}] (Rel. Int. [unitless])		
	Anti-periplanar [a]	Synclinal [a,c]		Anti-periplanar [b]	Synclinal [b]	
	Calc.	Calc.	Exp.	Calc.	Calc.	Exp. [h]
ν_1	2987	2988 (2994)	3014	0	1 (17)	2.0 (5)
ν_2	2965	2964 (2979)	2951	2	3 (50)	1.3 (22)
ν_3	2530	2582 (2604)	2607	1	0 (0)	0.5 (9)
ν_4	2261	2256 (2274)	2256	5	6 (100)	1.5 (26)
ν_5	1434	1426 (1435)	1419[d]	4	6 (100)	6.3 (100)
ν_6	1241	1254 (1258)	1249.7[d]	14	5 (83)	3.0 (45)
ν_7	1167	1195 (1200)	1193	1	2 (33)	0.8 (13)
ν_8	972	998 (956)	997	1	3 (50)	4.0 (67)
ν_9	878	921 (931)	926	1	5 (83)	7.0 (92)
ν_{10}	845	793 (788)	786	2	1 (17)	0.7 (11)
ν_{11}	709	694 (704)	701	1	5 (83)	3.7 (63)
ν_{12}	461	475 (484)	-	2	0	-
ν_{13}	346	351 (364)	[e]	1	0	-
ν_{14}	165	273 (203)	[e]	3	37	-
ν_{15}	247	193 (171)	[e]	7	21	-

[a] combined CCSD(T)/anharmonic B3LYP calculation, see equation (1)
[b] anharmonic B3LYP
[c] in parentheses, results of anharmonic CCSD(T) computations[1]
[d] two sites were observed with the most intense reported in the table (**Fig.1**)
[e] out of detection range
[f] Relative intensities given with respect to ν_5 located at 1419 cm^{-1} (experimental) rather than the most intense mode which is outside of our measurement range.
[g] None of the computed overtones has an intensity higher than 1 km mol^{-1} and are not reported
[h] lower limit of absolute intensity

Table 2A Comparison of predicted frequencies and intensities of Cl-CH_2-CN (CAN) along with experimental values measured in an Ar matrix.

Mode [f]	Symmetry	Freq. [cm^{-1}]		Freq. shift $^{35}Cl \rightarrow ^{37}Cl$ [cm^{-1}]		Int. [km mol^{-1}] (Rel. Int. [unitless])	
		Calc.[a]	Exp.	Calc.[b]	Exp.	Calc. [c]	Exp. [g]
ν_1	A'	2990	2972.1	0		4 (12)	2.3 (8)
ν_2	A'	2259	2263.4	0		0 (0)	0.6 (2)
ν_3	A'	1437	1431.1	0		5 (15)	5.1 (18)
ν_4	A'	1268	1271.1	0		18 (53)	9.3 (33)
ν_5	A'	929	930.8	0		15 (44)	24.9 (89)
ν_6	A'	750	745.4	-4	-4	34 (100)	28.0 (100)
ν_7	A'	476	484.2	-3	-3.5	5 (15)	2.1 (7)
ν_8	A'	181	[d]	-1		6 (17)	-
ν_9	A''	3020	3014.3	0		0 (0)	3.1 (11)
ν_{10}	A''	1183	1183.4	0		0 (0)	0.4 (1)
ν_{11}	A''	908	906.7	0		1 (0)	0.9 (3)
ν_{12}	A''	336	[d]	0		1 (0)	-

[a] combined CCSD(T)/anharmonic B3LYP calculation, see equation (1)
[b] harmonic CCSD(T)
[c] anharmonic B3LYP
[d] out of detection range
[e] relative intensities with respect to ν_6 at 745 cm^{-1}
[f] None of the computed overtones has an intensity higher than 1 km mol^{-1} and are not reported.
g)lower limit of the absolute intensities

Table 2B Comparison of predicted infrared frequencies and intensities of Cl-CH_2-NC, CAN-1 along with experimental values measured in an Ar matrix.

Mode		Freq. [cm^{-1}]		Freq. shift $^{35}Cl \rightarrow ^{37}Cl$ [cm^{-1}]		Rel. Int. [unitless]	Rel. Int. [unitless]
		Calc.[a]	Exp.	Calc.[b]	Exp.	Calc. [c]	Exp [e]
ν_1	A'	3002	3035.9	0		4	19
ν_2	A'	2137	2143.8	0		100	100
ν_3	A'	1457	1453.0	0		2	1
ν_4	A'	1311	1306.2	0		24	12
ν_5	A'	962	962.3	0		30	19
ν_6	A'	746	777.4	-4	-1.2	43	87
ν_7	A'	418	477.7	-3	-1.4	1	23
ν_8	A'	160	[d]	-1		2	-
ν_9	A''	3032	3036.0	0		0	19
ν_{10}	A''	1229	1228.2	0		1	1
ν_{11}	A''	951	-	0		0	-
ν_{12}	A''	242	[d]	0		0	-
Combination modes and overtones with intensities higher than 1 km × mol^{-1}							
$2\nu_5$		1908	-	0		1	-
$\nu_5+\nu_4$		2271	-	0		1	-
$\nu_6+\nu_3$		2202	2208.0	-5		6	1
$\nu_8+\nu_2$		2293	-	-1		1	-
$\nu_8+\nu_4$		1114	-	-1		1	-
$\nu_9+\nu_3$		4467	-	0		1	-
$\nu_{11}+\nu_{10}$		2180	2179.0	0		30	1
$\nu_{12}+\nu_2$		2370	-	0		1	-

[a] combined CCSD(T)/anharmonic B3LYP calculation, see equation (1)
[b] harmonic CCSD(T)
[c] anharmonic B3LYP, relative intensities with respect to ν_2 (178 km/mol)
[d] out of detection range
[e] relative intensities given with respect to ν_2

Table 2C Predicted infrared frequencies and intensities of HNCCHCl, CAN-2

Mode	Freq. [cm^{-1}] [a]	Freq. shift $^{35}Cl \rightarrow ^{37}Cl$ [cm^{-1}] [b]	Inten. [km mol^{-1}]
ν_1	3281	0	15
ν_2	3114	0	18
ν_3	2047	0	227
ν_4	1290	0	40
ν_5	1125	0	9
ν_6	1019	0	186
ν_7	837	0	67
ν_8	781	-4	34
ν_9	536	-1	39
ν_{10}	532	-3	2
ν_{11}	409	0	26
ν_{12}	182	-1	0
Combination modes and overtones with intensities higher than 1 km × mol^{-1}			
ν_1	6389	0	13
ν_2	6112	0	1
ν_3	4067	0	3
ν_6	2005	0	35
ν_8	1559	-7	1
ν_9	1078	-1	1
ν_{10}	1059	-6	5
$\nu_4+\nu_3$	3321	0	3
$\nu_6+\nu_3$	3071	0	2
$\nu_6+\nu_4$	2311	0	2
$\nu_6+\nu_5$	2145	0	8
$\nu_9+\nu_7$	1371	-1	7
$\nu_{10}+\nu_9$	1067	-4	1
$\nu_{11}+\nu_6$	1436	0	1
$\nu_{11}+\nu_7$	1249	0	1
$\nu_{11}+\nu_9$	943	-1	14
$\nu_{11}+\nu_{10}$	941	-3	2

[a] combined CCSD(T)/anharmonic B3LYP calculation, see equation (1)

[b] harmonic CCSD(T)

[c] anharmonic B3LYP results

Table 3 Rotational constants and dipole moment for selected isomers of CAN

	A_0/MHz	B_0/MHz	C_0/MHz	μ_e/D
CAN	25045	3109	2811	3.28
	25271.3583(45)[a)]	3150.74897(102)[a)]	2789.4927(22)[a)]	
CAN-1	25758	3327	2999	3.04
CAN-2	34114	2919	2705	1.89

a) ground state experimental values [82]

4.2 Spectroscopy

Prior to photolysis, the spectrum of pure HS-CH_2-CN in a noble gas matrix was recorded (**Fig. 2**) and analyzed. The measured IR band positions along with lower limits for absolute and relative intensities are presented in **Table 1** along with theoretically predicted values for synclinal and anti-periplanar forms (for structures of synclinal and anti-periplanar forms, see **Figure 1** from [83]).

Fig2 Experimental IR spectra of HS-CH_2-CN for pertinent regions of **Table 1**. Y scale is the intensity in arbitrary units.

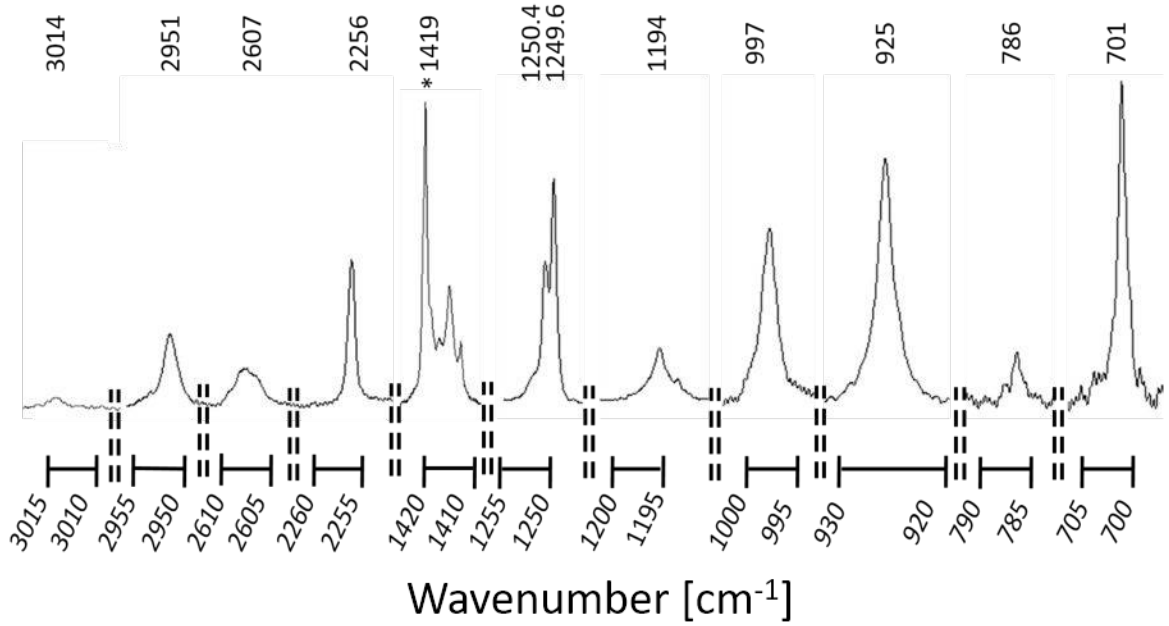

* all regions share a common y-scale except for the feature at 1419 cm^{-1} which has been reduced by a factor of 2.

Since HS-CH_2-CN is not a particularly rigid molecule, containing only a single, non-conjugated multiple bond, it might be expected to exhibit interesting site structures upon trapping in solid Ar or broadening due to allowed molecular motions within a matrix cage. However, IR absorption bands were narrow and only the peaks located near 1250 cm^{-1} and 1419 cm^{-1} had easily discernable structure. For the doublet near 1250 cm^{-1}, a typical ratio between components of 3:2 was observed with the higher intensity signal at 1249.6 cm^{-1}.

The absolute value of the difference between measured and predicted frequencies of the synclinal conformer ranges between 0 and 26 cm^{-1}. The sign of the difference depends on the band being considered. Overall, these deviations are generally 1% or less of the experimentally measured frequency. In light of considerable differences between HS-CH_2-CN as a pure liquid and in an Ar matrix environment, our matrix measurements are also remarkably consistent with reports for the pure liquid in the literature and reveal additional vibrations at 786, 1193, 1249.7, 1250.4, and 2607 cm^{-1} which have not yet been described (**Table 1 Supporting Information**).

Relative intensities were determined over the course of six experiments. Deviation of intensities for each vibration ranged between 4.9% and 10.6% (6.6% on average) for ten out of 11 bands. The highest frequency vibration (for which RSD was 30%) was excluded from this analysis as its very low intensity hindered proper peak integration. Absolute intensities measured for HS-CH_2-CN were consistently smaller than values predicted by calculations by a factor of 5 in five out of six experiments conducted. These errors are larger than would be expected based on determination of matrix thickness or peak integration for which the error should be around 9-11%. As these six experiments

were conducted using two different synthetic batches of the chemical (one experiment with the first batch and the five subsequent experiments with the second), this discrepancy is most likely due to partial decomposition of the second batch of HS-CH_2-CN during the vaporization and deposition. Work with this highly reactive compound was difficult. For this reason, we present the higher values obtained from the single experiment in **Table 1** that more closely match theoretical predictions. For this specific determination, measured absolute intensities vary from predicted values by factors between 0.5 and 4 depending on the band considered. The same goes for relative intensities which varied from predictions by factors between 0.7 and 3.8. Although this variation is significant, the pattern of intensities of the various bands qualitatively resembles one another when comparing experiment to theory.

Microwave studies indicate that HS-CH_2-CN can exist in either anti-periplanar or synclinal configurations in the gas phase at room temperature [83] and that these forms have an energy difference of 3.8±0.3 kJ/mol. Studies of L-isoserine [84] and β-alanine [85] indicate that it is sometimes possible to conserve ratios between conformers during matrix deposition. Based on the computed differences in vibrational frequencies of anti-periplanar and synclinal forms of HS-CH_2-CN (**Table 1**), the resolution of our spectrometer and observed peak widths, these conformers should be easily distinguishable in these measurements should they both become frozen in the Ar ice. The computed (CCSD(T)/cc-pVTZ) energetic difference between conformers is 4.5 kJ/mol, close to the experimental value, and indicate a 4.1 kJ/mol difference between conformer free enthalpies at room temperature. Assuming thermal equilibrium between isomers, a ratio of ~5:1 (synclinal to anti-periplanar) should be observed. However, no obvious sign

of their coexistence could be found in the measured spectra. Measured IR frequencies are in better agreement with what is predicted for the synclinal form, the more stable of the two conformations. As the absolute intensities are low for both compounds and IR signals from the most stable isomer were already small, it may be that we were simply unable to detect bands of the less abundant anti-periplanar conformer.

The Cl-CH_2-CN purchased for these experiments had excellent purity and identification of peaks was unambiguous based on previous reports. Comparison between calculated and experimentally determined values of intensities and position of peaks of Cl-CH_2-CN are presented in **Table 2A**. The experimental IR spectrum of Cl-CH_2-CN is presented in **Fig 3**. Most peaks appear as overlapping doublets suggesting existence of at least two different matrix sites. In **Table 2A**, the more intense member of the doublet is reported. For the v_6 and v_7 vibrations a quartet is observable. For v_6, peaks at 745 and 755 cm^{-1} are assigned to the two matrix sites of ^{35}Cl-CH_2-CN and the less intense peaks at 741 and 751 cm^{-1} were attributed to matrix sites of the ^{37}Cl-CH_2-CN isomer. For v_7, more intense features at 484 and 483 cm^{-1} were again assigned to ^{35}Cl-CH_2-CN and the smaller 482 and 481 cm^{-1} bands to ^{37}Cl-CH_2-CN.

Fig3 Experimental IR spectra of Cl-CH_2-CN (see **Table 2A**). Y scale is the intensity in arbitrary units.

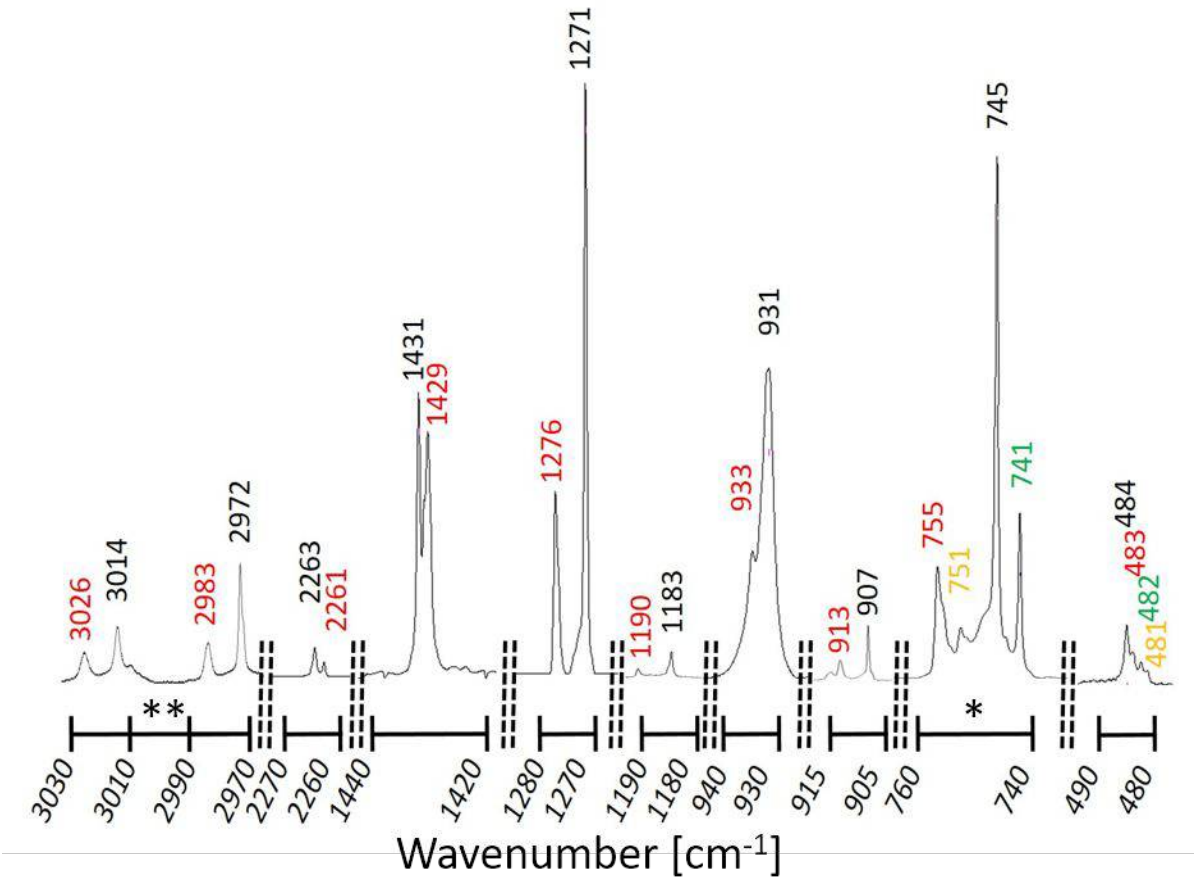

Matrix sites assigned to ^{35}Cl-CH_2-CN (black and red) and matrix sites for ^{37}Cl-CH_2-CN (green and yellow). * all regions share a common y-scale except for the region between 740 cm^{-1} and 760 cm^{-1} which was reduced by a factor of 2. **all regions share the same x scale except for the region between 3030 cm^{-1} and 3010 cm^{-1} which was reduced by a factor of 2

Comparing theoretically predicted values of IR absorption frequencies to experimentally observed values, differences range between 0.4 and 18 cm^{-1} with the sign of the deviation varying depending on the mode being considered. This amounts to less than 1% of the measured value for all modes except for that for ν_7 at 476 cm^{-1} which differs by ~1.7%. The position of vibrations was also very similar to previously reported in liquid and in gas phase and ranges between 0 and 14 cm^{-1} (**Table 2 Supporting**

Information). We were not able to detect any of the overtones or combinations reported in the work of Zeil et al.[27]. Our inability to observe such features is consistent with our calculations which indicate they should have very low intensities. While no new features of this molecule were detected in our study, no author has reported vibrations from ^{37}Cl-CH_2-CN isotopomer or peak locations in a noble gas matrix.

Measured absolute intensities are again smaller than theoretical predictions, although they are much closer than those measured for HS-CH_2-CN. Measured values are only smaller than theoretical values by up to a factor of around 2.4 depending on the band being considered. Better agreement likely has to do with the higher purity and stability of the commercially available chemical.

Absolute intensities have been measured previously in the liquid phase by Nemes et al.[38] and by Thomas et al.[39] for the CN vibration. They are several times larger than both our experimental and calculated values. Absolute intensities were also calculated by Wladkowski et al.[36]. Despite their moderate level of theory, their values are quite similar to our own.

4.3 Photochemistry

HS-CH_2-CN was irradiated using either 248 or 193 nm laser light and the results of photolyses at these wavelengths are given in **Table 4** and include photoproduct peak positions, intensities, behavior upon annealing, and assignments. Arrows in the anneal column indicate whether the intensity of a given peak in the IR spectrum increased (up) or decreased (down) following annealing. Intensity values are given relative to the highest

intensity photoproduct peak (a value of 100) to provide information about ease of detection of various products as well as peak ratios for bands assigned to the same photoproduct. Values of intensities are based on their integrals.

Table 4 Peaks observed after HS-CH_2-CN laser photolysis.

Freq. [cm^{-1}]	anneal	Rel. Int [a] [unitless] photolysis 248 nm	Rel. Int. [a] [unitless] photolysis 193 nm	Assignment
3611	↓	32	9	
3233	↓	47	-	HC-CN
3219	↓	29	69	
3162	↓	-	100	
2168	↓	3	2	CH_3SCN
2142	↓	88	17	CH_3NSC
2091	↓	9	34	
2050	↓	-	8	CH_3SNC
2024	↓	18	6	
1930	↑	9	2	
1897	↓	-	3	
1888	↓	-	6	
1735	↓	12	-	HC-CN
1528	↑	29	2	CS_2
1328	↓	-	34	
1309	↓	12	22	CH_4
1289	↓	6	59	HS-CH_2-NC
1148	↓	-	2	
1123	↓	-	2	
1063	↓	6	-	H_2C-CN/CH_2=S
996	↓	100	-	CH_2=S
993	↓	76	-	CH_2=S
936	↓	11	2	HS-CH_2-NC
802	↓	-	13	
777	↑	4	6	
723	↓	12	50	
687	↓	29	-	H_2C-CN
617	↓	-	3	CH_3* tentative detection
483	↓	3	-	HC-CN

A variety of photoproducts were at least tentatively identified, some of which were common across photolysis wavelength and others of which were not. Formation of mercaptoisocyanomethane (HS-CH_2-NC) was observed at both wavelengths with reasonable certainty and features associated with this species are shown in **Fig 4** with positions listed in **Table 5**. Three peaks were associated with this species whose relative ratio is conserved across multiple experiments, suggesting that they belong to a single photoproduct. While these features are not strong, the agreement of observed line positions and intensities with *ab initio* theoretical results [1] for HS-CH_2-NC (**Table 5**) form a good basis for attribution of these features. The prevalence of CN/NC conversion observed for other cyanide containing carbon chain molecules in a matrix environment also lead us to expect that this transformation will occur.

Fig4 Experimental IR spectrum of HS-CH_2-NC formed as a photoproduct in an Ar matrix. Y scale is the intensity in arbitrary units.

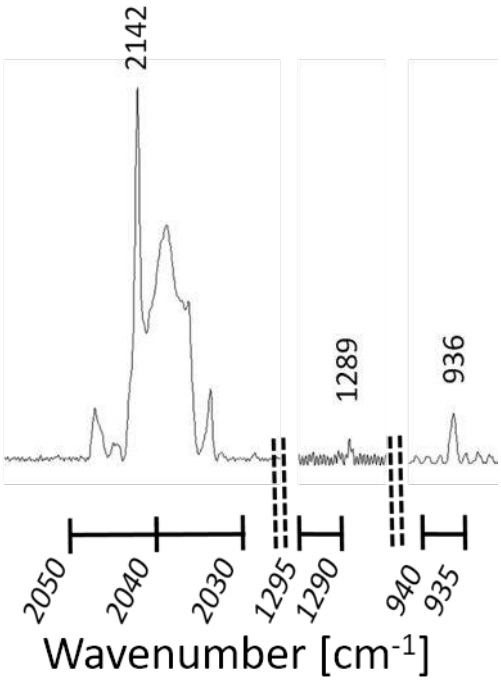

Table 5 Comparison of predicted infrared frequencies and intensities of HS-CH_2-NC with experimental values

Mode	Frequency [cm^{-1}]		Rel. Int. [unitless]	
	Calc[a].	Exp.	Calc.[b]	Exp.
ν1	2998	-	0	-
ν2	2993	-	2	-
ν3	2670	-	0	-
ν4	2135	2142	100	100
ν5	1458	-	4	-
ν6	1294	1288.9	15	7
ν7	1247	-	4	-
ν8	1030	-	1	-
ν9	939	935.9	19	12
ν10	804	-	1	-
ν11	702	-	9	-
ν12	416	-	1	-
ν13	297	-	3	-
ν14	278	-	6	-
ν15	171	-	2	-

a) combined CCSD(T)/anharmonic B3LYP calculation, see equation (1) and Ref. 1
b)relative intensities with respect to v4 at 2142 cm^{-1}

Photoisomerization of HS-CH_2-CN into the more stable methyl thiocyanate (CH_3SCN) and methyl isothiocyanate (CH_3NCS) are also likely processes in a matrix environment. Although not presented here, we compared our HS-CH_2-CN photoproduct spectra with those of pure CH_3SCN and CH_3NCS isolated in Ar (work in preparation [86]). The calculated and measured absolute intensities of IR bands of those two molecules are far larger than for HS-CH_2-CN or HS-CH_2-NC and, as a consequence, even a small amount of CH_3NCS or CH_3SCN formed via photolysis should be easily detectable.

The most stable C_2H_3SN isomer, CH_3NCS, has its most intense vibrations at 2142 cm^{-1} and 1419 cm^{-1} with a ratio of 100 to 6 [86]. While we were able to distinguish a 2142 cm^{-1} vibration, this was assigned to HS-CH_2-NC. A band of the parent molecule falls in the exact location of the 1419 cm^{-1} feature. While we cannot rule out the formation of this species, it is impossible to confirm its production here.

Positive identification of the second isomer, CH_3SCN is also problematic. Peaks located at 2168 cm^{-1}, 1442 cm^{-1}, and 2951 cm^{-1} (with a ratio of intensities of 3:1:1) should be distinguishable[86]. While there is photolytic formation of a species with a vibration at 2168 cm^{-1} which might be linked to CH_3SCN, this peak had a very small intensity in all five photolysis experiments performed. The other two vibrations were not observable and may simply have been below the signal-to-noise limit. Stronger evidence is needed to confirm production of CH_3SCN.

Some information exists concerning the potential production of the higher energy isomers CH_3CNS and CH_3SNC which were not available commercially or through synthesis. CH_3CNS is likely not formed as the most intense peak, located at 2230 cm^{-1} [86], could not be detected.

CH_3SNC has an experimentally assigned vibration at 2050 cm^{-1} accompanied by a smaller feature at 1442 cm^{-1} (intensity ratio of 100:9)[86]. Although a vibration at 2050 cm^{-1} is often produced following 193 nm photolysis the second vibration at 1442 cm^{-1} is very close to our limit of detection. Without stronger evidence, CH_3SNC detection cannot be confirmed.

The remainder of products observed for this system requires cleavage of at least one bond and separation of the resulting fragments into their own respective matrix cages

to be produced. For instance, evidence for formation of $H_2C=S$ following 248 nm irradiation suggests that at least some C-C bond cleavage occurs. This photolytic product was identified on the basis of its three most intense bands which were measured previously in an Ar matrix [58]. No $H_2C=S$ was observed following 193 nm irradiation. It may be that the higher photon energy promoted swift loss of the H-atoms from H2C=S to form CS (followed by CS conversion to CS_2).

H_2C-CN and HC-CN, were likely formed following 248 nm irradiation but not following 193 nm exposure. Both were previously measured in Ar matrix environment, HC-CN by Dendramis et al. and by Maier et al. [87, 88] and H_2C-CN by Cho et al. [89]. HC-CN was identified in this work as a product on the basis of three unambiguous peaks. For H_2C-CN, one peak was unambiguous while a second was very near the limit of detection (not included in table 5). A third peak which should also be visible shares the same location as a band of $H_2C=S$. Overall, detection of H_2C-CN is less certain than HC-CN.

Formation of both HC-CN and H_2C-CN requires cleavage of the S-C bond of HS-CH_2-CN. Given that both HC-CN and H2C-CN were observed, It is reasonable to assume that some HS or H_2S (possibly formed by an escaping HS taking with it another H-atom) might also be detectable. However, based on IR observations of HS and H_2S in an Ar matrix environment [90], there is no evidence of the formation of either of these in any of the photolyses performed here.. The photochemistry of Ar matrix isolated H_2S and HS have been studied[91-93] and H_2S photolysis leads to production of HS followed eventually by atomic sulfur formation. While we have evidence of production of atomic sulfur, from our experiments, described later in discussion of CS_2 formation and annealing, we cannot say whether its production proceeds through H_2S and/or HS, some other intermediate, or

through sequential scission of H atom and then S atom from the H-S-CH_2CN parent.

A number of other products were also observed at both photolysis wavelengths suggesting that cleavage of single bonds is quite facile and that escape of the fragments thus produced from the matrix cage is also probable. Methane formation, identified here based on comparison with prior measurements in an Ar matrix [58], requires cleavage of both S-C and C-C bonds as well as at least one free H atom coming from another matrix site or the possible presence of complexes in a single site. While H atom migration is not a surprising process in a noble gas matrix environment, the formation of CS_2 (identified as compared to measurements in Ar matrix by Szczepanski et al.[94]), possibly from CS and S, requires sulfur atoms coming from two different matrix cages or two parent molecules. This suggests either that free S atoms are somewhat mobile in an Ar matrix, that adjacent matrix sites were near enough to allow minimally mobile S atoms to find one another following photolysis, or a reasonable abundance of HS-CH_2-CN dimers or larger complexes exist in the matrix. Finally, CH_3 identified based on IR measurements in Ar matrix by Pacansky et al. and by Snelson et al. [95,96], was observed upon irradiation at 193 nm but not following exposure to 248 nm. Given the presence of CH_4, production of CH_3 is logical upon exposure to higher energy photon radiation.

Some peaks remain unassigned. Intense peaks, for which we did not find any convincing attribution are marked in the **Table 5**. These lines do not fit with other potential products whose IR signatures in an Ar matrix environment have already been reported: S=CHCN[97]; CH_3CN[98] or further photolysis products (CH_3NC, CH_2NCH, CH_2CNH, CH_2NC)[98]; CH_3SH[58]; HS[90]; H_2S[90]; CH_2 (NIST gas)**;** HS-CN[99]; or HS-NC[99].

We also performed photolysis of Cl-CH_2-CN using 193 nm laser light. As no UV-

VIS spectrum of Cl-CH_2-CN is available in the literature, we measured it and found no clear absorption bands between 200 nm and 900 nm, suggesting that two-photon processes were involved in photolysis.

The main photolysis product of Cl-CH_2-CN photolysis was Cl-CH_2-NC.

The position and intensities of peaks of FTIR measurements were compared with theoretical calculations and are presented in **Table 2b** and in **Fig5**. The yield of this product was high enough that ^{37}Cl isotopomers for v_6 and v_7 vibrations could be discerned at 775.5 cm^{-1} and 476.3 cm^{-1}, with intensities proportional to the ratio of natural abundances of ^{35}Cl and ^{37}Cl. Additionally, a few small overtone vibrations could be distinguished in the spectra ($\nu_6+\nu_3$ at 2208.0 cm^{-1} and $\nu_{11}+\nu_{10}$ at 2179.0 cm^{-1}). The anharmonic computations predicted that both these modes are in resonance with very intense v_2. It seems that, the intensities of those combinational modes are overestimated, but the precise prediction for resonance are far beyond the applied theoretical methods. Vibrations at 2144.7 cm^{-1}, 1228.9 cm^{-1} and 960.6 cm^{-1} are likely matrix sites of Cl-CH_2-NC. Apart from features assigned to the Cl-CH_2-NC product, only six peaks remain unassigned (see **Fig 6**): 1982.4 cm^{-1} (with shoulder centered at 1981.cm^{-1}); 1406.0 cm^{-1} (with shoulder centered at 1406.9 cm^{-1}); 1390.4 cm^{-1}, 1387.8 cm^{-1}, 622.8 cm^{-1} and 617.2 cm^{-1}. No good evidence for formation of CAN 2 (HNCCHCl) was found (see calculations **Table 2C**).

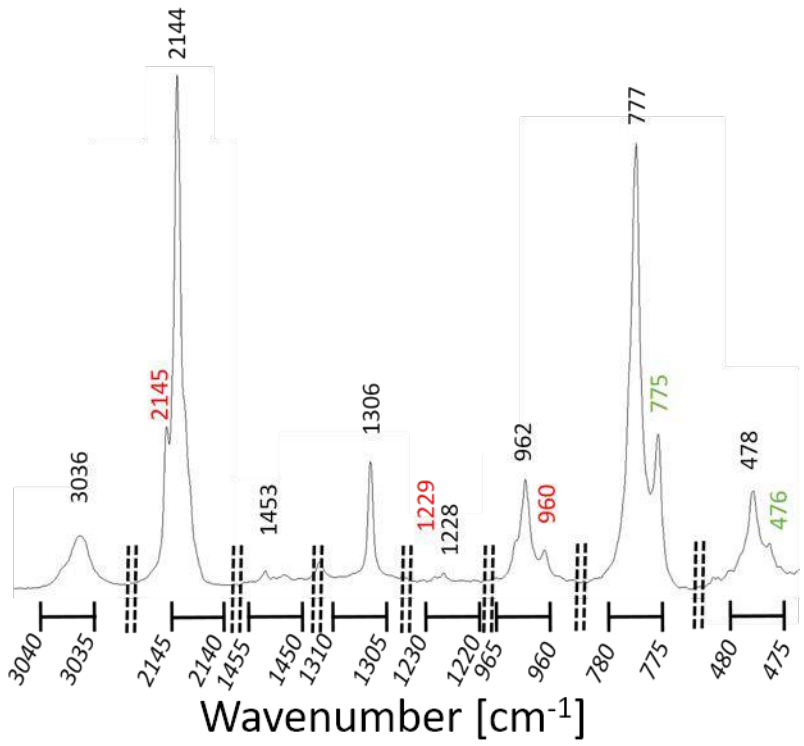

Fig 5 Experimental IR spectrum of Cl-CH_2-NC. Matrix sites assigned to ^{35}Cl-CH_2-CN (black and red) and ^{37}Cl-CH_2-CN (green) . Y scale is the intensity in arbitrary units.

* all regions share common x- and y-scales

Fig 6 Unidentified peaks produced during Cl-CH_2-CN photolysis (red labels) along with 475-480cm^{-1} region (black and green labels) to enable comparison of intensities with **Fig 5**. . Y scale is the intensity in arbitrary units.

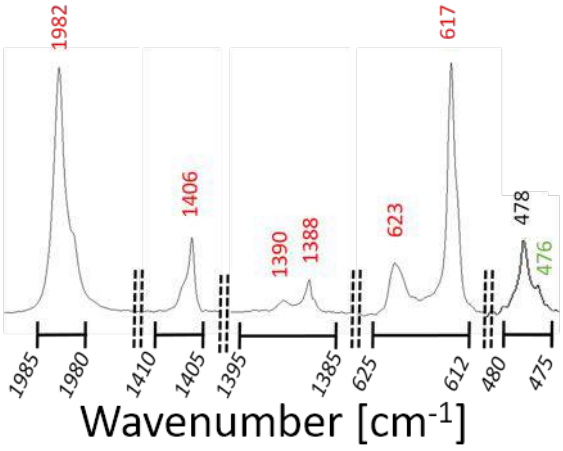

As S atoms and H atoms seemed to be produced on photolysis of HS-CH_2-CN, it is possible that Cl atom and H atom may be produced upon photolysis of Cl-CH_2-CN. Hydrochloric acid (HCl) is the simplest molecule containing these atoms and, although spectra of Ar matrix isolated HCl are available in the literature, we repeated experiments in a noble gas matrix in the hopes of ruling out HCl or HCl complexes as photoproducts. Our measurements of HCl deposited in Ar matrix match with other published values of the position of the monomer band of HCl in those conditions[100],[101],[102],[103],[104] except for a peak located at 1981.9 cm^{-1} (compare with **Fig 7**). This is very close to a feature observed following 193 nm photolysis of Cl-CH_2-CN at 1982.4 cm^{-1}, unaccompanied by the main HCl monomer band or bands of any other HCl complex. In terms of HCl measurements, this feature was not present in the gas phase and is not caused by impurities in the HCl sample (samples from different suppliers all exhibited the same feature), noble gas impurities (Ar and Kr both show production of a feature near this location), corrosion of the deposition line (both metal and glass manifolds lead to the same result), or reaction

with deposition window (CsI and sapphire deposition windows also showed the same vibrations). As this peak is not mentioned in the literature either as a band of HCl isolated in a rare gas matrix or as a product of HCl complexation with water or some other species, we take the opportunity to report its presence here.

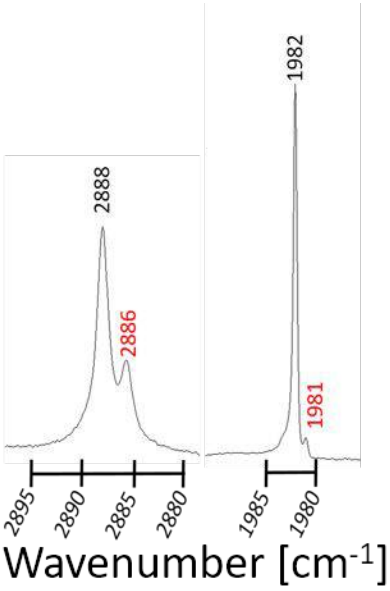

Fig7 Selected regions depicting bands of HCl in an Ar matrix (ratio 1:1000). Red labels are matrix sites. Y scale is the intensity in arbitrary units.

4.4 Annealing

The last step of sample processing was annealing. During annealing, softening of the noble gas matrix can allow some isolated, reactive species to become mobile and recombine, possibly emitting light in the process, and allow changes in specific matrix sites that might be visible in subsequent IR spectra. Aside from confirming photoproduct assignment using IR spectra, we also monitored for light emission during annealing using a low resolution CCD spectrometer. Following 193 nm irradiation of HS-CH_2-CN, three different emission signals were observed, one starting at around 8 K, a second between 8 and 12 K, and a third above 12 K. Just above 8K, we were able to see a greenish glow (a broad weak line at 521 nm) (**Fig8**).

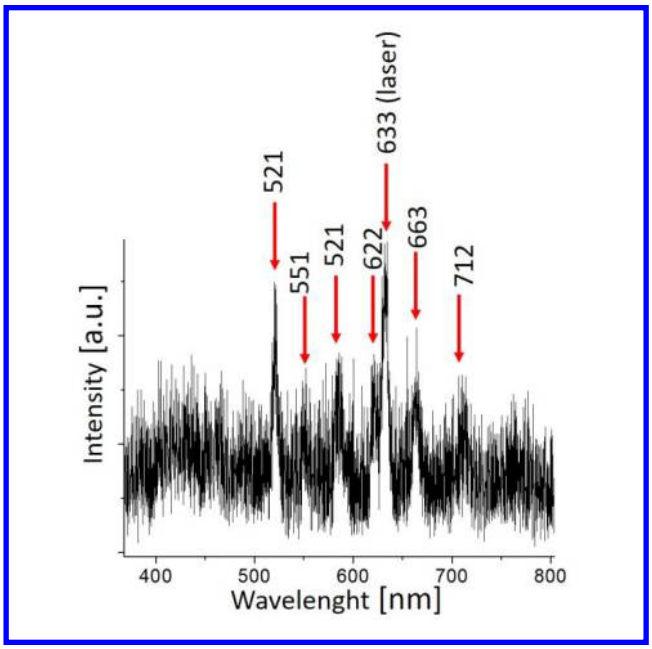

Fig8 Glow after photolysis of HS-CH_2-CN at 10K

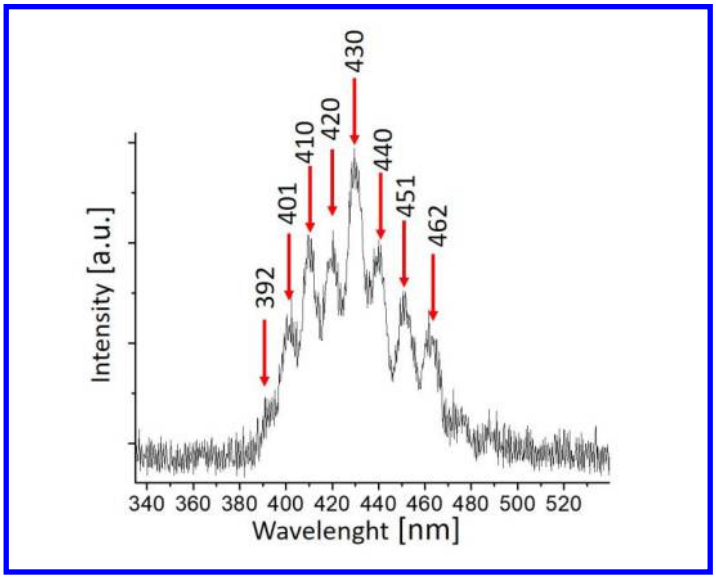

Fig9 Glow after photolysis of HS-CH_2-CN at 20 K assigned to OCS

Although we do not have any explanation for this emission, annealing of the photolysed sample of Cl-CH_2-CN also produced this greenish glow which allows us to conclude that it is not related to the presence of sulfur. When heating photolysed samples of HS-CH_2-CN between 8K and 10K, additional glows at 551, 586 nm, 622 nm, 663 nm and 712.5 nm (**Fig8**) appeared. We attribute this progression to SO (c $^1\sum^- \rightarrow$ a $^1\Delta$) emission[105].

Excited SO is produced through the reaction between ground state S($^3P_2$) and O($^3P_2$) atoms where the main source of atomic oxygen in our sample may be photolysis of CO_2 into CO and O. Above 12 K, a large amount of sulfur (^3P) was mobilized[106]. Recombination with CO(X1∑+) forms electronically excited OCS and produces a bluish afterglow with vibrational spacing of around 550 cm^{-1} and maximum at 430 nm (see **Fig 9**). The glow persists up to 25 K. The temperature separation of SO and OCS emission is likely a consequence of the larger mobility of atomic oxygen compared with sulfur in an Ar matrix which allows it to become mobile at a lower temperature.

5. Conclusions

We have investigated the photochemistry of mercaptoacetonitrile (HS-CH_2-CN) and chloroacetonitrile (Cl-CH_2-CN) in noble gas (Ar) matrices at 6K. We determined position and intensities of peaks and supported our conclusions with computational analysis. For both, isocyanide compounds (HS-CH_2-NC and Cl-CH_2-NC) were identified. While no products indicating ejection of Cl or other moieties from the matrix cage were identified for Cl-CH_2-CN, evidence exists for a variety of processes in the case of HS-CH_2-CN. For example, production of CS_2 following photolysis and observation of emission by SO and OCS upon subsequent annealing suggest formation of a mobilized free sulfur atom upon photolysis of HS-CH_2-CN. Observation of CH_2-CN and CH-CN show loss of HS. The formation of CH_2=S indicate the loss of CN while production of CH_4 provide evidence for the loss of both HS and CN.

Supporting information

Tables with comparison of results of this work with previous reports for $HSCH_2CN$ and for $ClCH_2CN$

Acknowledgments

This work was supported by NCN grant 2015/17/B/ST4/03875.

J.-C. G. thanks the Centre National d'Etudes Spatiales (CNES) and the French Programme National "Physique et Chimie du Milieu Interstellaire" for financial support.

Reference list:

1. Gronowski, M.; Turowski, M.; Custer, T.; Kołos, R., A Theoretical Study on the Spectroscopy, Structure, and Stability of C_2H_3NS Molecules. *Theoretical Chemistry Accounts* **2016,** *135* (9), 222.
2. Gibb, E.; Nummelin, A.; Irvine, W. M.; Whittet, D. C. B.; Bergman, P., Chemistry of the Organic-Rich Hot Core G327.3–0.6. *The Astrophysical Journal* **2000,** *545* (1), 309.
3. Frerking, M.; Linke, R.; Thaddeus, P., *Interstellar isothiocyanic acid*. 1980; Vol. 234.
4. Halfen, D. T.; Ziurys, L. M.; Brünken, S.; Gottlieb, C. A.; McCarthy, M. C.; Thaddeus, P., Detection of a New Interstellar Molecule: Thiocyanic Acid HSCN. *The Astrophysical Journal Letters* **2009,** *702* (2), L124.
5. Nayak, M. K.; Chaudhuri, R. K.; Krishnamachari, S. N. L. G., Theoretical study on the excited states of HCN. *The Journal of Chemical Physics* **2005,** *122* (18), 184323.
6. Thiel, V.; Belloche, A.; Menten, K. M.; Garrod, R. T.; Müller, H. S. P., Complex organic molecules in diffuse clouds along the line of sight to Sagittarius B2. *Astronomy & Astrophysics* **2017,** *605*.
7. Danger, G.; Rimola, A.; Abou Mrad, N.; Duvernay, F.; Roussin, G.; Theule, P.; Chiavassa, T., Formation of hydroxyacetonitrile (HOCH2CN) and polyoxymethylene (POM)-derivatives in comets from formaldehyde (CH2O) and hydrogen cyanide (HCN) activated by water. *Physical Chemistry Chemical Physics* **2014,** *16* (8), 3360-3370.
8. Zeng, S.; Quénard, D.; Jiménez-Serra, I.; Martín-Pintado, J.; Rivilla, V. M.; Testi, L.; Martín-Doménech, R., First detection of the pre-biotic molecule glycolonitrile (HOCH2CN) in the interstellar medium. *Monthly Notices of the Royal Astronomical Society: Letters* **2019,** *484* (1), L43-L48.
9. Wakelam, V.; Hersant, F.; Herpin, F., Sulfur Chemistry: 1d Modeling in Massive Dense Cores. *Astronomy & Astrophysics* **2011,** *529*, A112.
10. Liu, H. B.; Jiménez-Serra, I.; Ho, P. T. P.; Chen, H.-R.; Zhang, Q.; Li, Z.-Y., Fragmentation and Ob Star Formation in High-Mass Molecular Hub-Filament Systems. *The Astrophysical Journal* **2012,** *756* (1), 10.
11. Li, J.; Wang, J.; Zhu, Q.; Zhang, J.; Li, D., Sulfur-Bearing Molecules in Massive Star-Forming Regions: Observations of Ocs, Cs, H2s, and So. *The Astrophysical Journal* **2015,** *802* (1), 40.
12. Esplugues, G. B.; Viti, S.; Goicoechea, J. R.; Cernicharo, J., Modelling the Sulphur Chemistry Evolution in Orion Kl. *Astronomy & Astrophysics* **2014,** *567*, A95.
13. Woods, P. M.; Occhiogrosso, A.; Viti, S.; Ka uchova, Z.; Palumbo, M. E.; Price, S. D., A New Study of an Old Sink of Sulphur in Hot Molecular Cores: The Sulphur Residue. *Monthly Notices of the Royal Astronomical Society* **2015,** *450* (2), 1256-1267.
14. Linke, R. A.; Frerking, M. A.; Thaddeus, P., Interstellar Methyl Mercaptan. *The Astrophysical Journal* **1979,** *234*, L139.
15. Gibb, E.; Nummelin, A.; Irvine, W. M.; Whittet, D. C. B.; Bergman, P., Chemistry of the Organic-Rich Hot Core G327.3−0.6. *The Astrophysical Journal* **2000,** *545* (1), 309-326.
16. Wakelam, V.; Loison, J. C.; Herbst, E.; Pavone, B.; Bergeat, A.; Béroff, K.; Chabot, M.; Faure, A.; Galli, D.; Geppert, W. D.; Gerlich, D.; Gratier, P.; Harada, N.; Hickson, K. M.; Honvault, P.; Klippenstein, S. J.; Picard, S. D. L.; Nyman, G.; Ruaud, M.; Schlemmer, S.; Sims, I. R.; Talbi, D.; Tennyson, J.; Wester, R., The 2014 Kida Network for Interstellar Chemistry. *The Astrophysical Journal Supplement Series* **2015,** *217* (2), 20.
17. Goicoechea, J. R.; Pety, J.; Gerin, M.; Teyssier, D.; Roueff, E.; Hily-Blant, P.; Baek, S., Low Sulfur Depletion in the Horsehead Pdr. *Astronomy and Astrophysics* **2006,** *456* (2), 565-580.
18. Fayolle, E. C.; Öberg, K. I.; Jørgensen, J. K.; Altwegg, K.; Calcutt, H.; Müller, H. S. P.; Rubin, M.; van der Wiel, M. H. D.; Bjerkeli, P.; Bourke, T. L.; Coutens, A.; van Dishoeck, E. F.; Drozdovskaya, M. N.; Garrod, R. T.; Ligterink, N. F. W.; Persson, M. V.; Wampfler, S. F.; Balsiger,

H.; Berthelier, J. J.; De Keyser, J.; Fiethe, B.; Fuselier, S. A.; Gasc, S.; Gombosi, T. I.; Sémon, T.; Tzou, C. Y.; the, R. t., Protostellar and cometary detections of organohalogens. *Nature Astronomy* **2017,** *1* (10), 703-708.
19. Öberg, K. I., Photochemistry and Astrochemistry: Photochemical Pathways to Interstellar Complex Organic Molecules. *Chemical Reviews* **2016,** *116* (17), 9631-9663.
20. d'Hendecourt, L.; Dartois, E., Interstellar matrices: the chemical composition and evolution of interstellar ices as observed by ISO. *Spectrochimica Acta Part A: Molecular and Biomolecular Spectroscopy* **2001,** *57* (4), 669-684.
21. Møllendal, H.; Samdal, S.; Guillemin, J.-C., Rotational Spectrum, Conformational Composition, Intramolecular Hydrogen Bonding, and Quantum Chemical Calculations of Mercaptoacetonitrile (HSCH2C≡N), a Compound of Potential Astrochemical Interest. *The Journal of Physical Chemistry A* **2016,** *120* (12), 1992-2001.
22. Bacchus-Montabonel, M.-C., Proton-induced collision dynamics on potential prebiotic sulfur species. *Physical Chemistry Chemical Physics* **2018,** *20* (14), 9084-9089.
23. Mathias, E.; Shimanski, M., Synthesis of mercaptoacetonitrile under mild conditions. *Journal of the Chemical Society, Chemical Communications* **1981,** (11), 569-570.
24. Wepplo, P., Synthesis of Mercaptoacetonitrile and Cyanomethyl Thioesters. *Synthetic Communications* **1989,** *19* (9-10), 1533-1538.
25. Gaumont, A. C.; Wazneh, L.; Denis, J. M., Thiocyanohydrins, a New Class of Compounds, Precursors of Unstabilized Thiocarbonyl Derivatives. *Tetrahedron* **1991,** *47* (27), 4927-4940.
26. Alexander, S. R.; Fairbanks, A. J., Direct aqueous synthesis of cyanomethyl thioglycosides from reducing sugars; ready access to reagents for protein glycosylation. *Organic & Biomolecular Chemistry* **2016,** *14* (28), 6679-6682.
27. Zeil, v. W., Die Schwingungsspektren der chlorierten Acetonitrile. In *Zeitschrift für Physikalische Chemie*, 1958; Vol. 14, p 230.
28. Durig, J. R.; Wertz, D. W., Far infrared and Raman spectra of the haloacetonitriles. *Spectrochimica Acta Part A: Molecular Spectroscopy* **1968,** *24* (1), 21-29.
29. Jones, R. G.; Orville-Thomas, W. J., 862. Spectroscopic studies. Part V. The spectra and structure of monohalogenoacetonitriles. *Journal of the Chemical Society (Resumed)* **1965,** (0), 4632-4646.
30. van Der Kelen, G. P., Studies on Halogenated Aliphatic Compounds VII. Dipole Moments and Infrared Spectra of Halogenated Acetonitriles. *Bulletin des Sociétés Chimiques Belges* **1962,** *71* (7-8), 421-430.
31. Allerhand, A.; von Rague Schleyer, P., Nitriles and Isonitriles as Proton Acceptors in Hydrogen Bonding: Correlation of ΔvOH with Acceptor Structure. *Journal of the American Chemical Society* **1963,** *85* (7), 866-870.
32. Schumann, H.; Speis, M.; Bosman, W. P.; Smits, J. M. M.; Beurskens, P. T., Monosubstituted nitrogen donors as ligands in cyclopentadienyliron complexes: synthesis, reactivity, ligand properties, and crystal structure of [C5H5Fe(CO)2(C5H5N)]SbF6. *Journal of Organometallic Chemistry* **1991,** *403* (1), 165-182.
33. Augdahl, E.; Klaboe, P., Spectrocopic studies of charge transfer complexes—VI: Nitriles and iodine monochloride. *Spectrochimica Acta* **1963,** *19* (10), 1665-1673.
34. Butt, G.; Cilmi, J.; Hoobin, P. M.; Topsom, R. D., The transmission of resonance effects through a methylene group—spectroscopic studies on some α-substituted-acetonitriles and p-toluonitriles. *Spectrochimica Acta Part A: Molecular Spectroscopy* **1980,** *36* (6), 521-524.
35. Crowder, G. A., Force constants and normal vibrations of the haloacetonitriles. *Molecular Physics* **1972,** *23* (4), 707-715.
36. Wladkowski, B. D.; Lim, K. F.; Allen, W. D.; Brauman, J. I., The SN2 identity exchange reaction ClCH2CN + Cl- .fwdarw. Cl- + ClCH2CN: experiment and theory. *Journal of the American Chemical Society* **1992,** *114* (23), 9136-9153.
37. Nemes, L.; Orville-Thomas, W. J., Infra-red dispersion studies. Part 3.—Band intensities

of acetonitrile and its chlorinated derivatives. *Transactions of the Faraday Society* **1965,** *61* (0), 1839-1849.
38. Nemes, L.; Orville-Thomas, W. J., Infra-red dispersion studies. Part 5.—Variation of intensity with change of phase for acetonitrile and its chlorinated derivatives. *Transactions of the Faraday Society* **1965,** *61* (0), 2612-2622.
39. Thomas, B. H.; Orville-Thomas, W. J., Infrared intensities of V(C□N) bands. *Journal of Molecular Structure* **1971,** *7* (1), 123-135.
40. George, W. O.; Hirani, P. K.; Lewis, E. N.; Maddams, W. F.; Williams, D. A., Aggregation and association of polar molecules in low temperature matrices and in the gaseous phase. *Journal of Molecular Structure* **1986,** *141*, 227-236.
41. Apkarian, V. A.; Schwentner, N., Molecular Photodynamics in Rare Gas Solids. *Chemical Reviews* **1999,** *99* (6), 1481-1514.
42. E. Bondybey, V.; Räsänen, M.; Lammers, A., Chapter 10. Rare-gas matrices, their photochemistry and dynamics: recent advances in selected areas. *Annual Reports Section "C" (Physical Chemistry)* **1999,** *95* (0), 331-372.
43. Kołos, R.; Sobolewski, A. L., The Infrared Spectroscopy of Hnccc: Matrix Isolation and Density Functional Theory Study. *Chemical Physics Letters* **2001,** *344* (5-6), 625-630.
44. Kawaguchi, K.; Ohishi, M.; Ishikawa, S.-I.; Kaifu, N., Detection of Isocyanoacetylene HCCNC in TMC-1. *The Astrophysical Journal* **1992,** *386*, L51-L53.
45. Kawaguchi, K.; Takano, S.; Ohishi, M.; Ishikawa, S.-I.; Miyazawa, K.; Kaifu, N.; Yamashita, K.; Yamamoto, S.; Saito, S.; Ohshima, Y.; Endo, Y., Detection of HNCCC in TMC-1. *The Astrophysical Journal* **1992,** *396*, L49-L51.
46. Gensheimer, P. D., Observations of HCCNC and HNCCC in IRC+10216. *Astrophysics and Space Science* **1997,** *251* (1), 199-202.
47. Vastel, C.; Kawaguchi, K.; Quénard, D.; Ohishi, M.; Lefloch, B.; Bachiller, R.; Müller, H. S. P., High spectral resolution observations of HNC3 and HCCNC in the L1544 pre-stellar core. *Monthly Notices of the Royal Astronomical Society: Letters* **2018,** *474* (1), L76-L80.
48. Coupeaud, A.; Turowski, M.; Gronowski, M.; Pietri, N.; Couturier-Tamburelli, I.; Kołos, R.; Aycard, J. P., Spectroscopy of Cyanodiacetylene in Solid Argon and the Photochemical Generation of Isocyanodiacetylene. *Journal of Chemical Physics* **2007,** *126* (16), 164301.
49. Smith, A. M.; Schallmoser, G.; Thoma, A.; Bondybey, V. E., Infrared spectral evidence of N≡C–C≡C–N≡C: Photoisomerization of N≡C–C≡C–C≡N in an argon matrix. *The Journal of Chemical Physics* **1993,** *98* (3), 1776-1785.
50. Kołos, R., Photolysis of dicyanodiacetylene in argon matrices. *Chemical Physics Letters* **1999,** *299* (2), 247-251.
51. Kołos, R.; Waluk, J., Matrix-Isolated Products of Cyanoacetylene Dissociation. *Journal of Molecular Structure* **1997,** *408-409*, 473-476.
52. Callear, A. B.; Dickson, D. R., Transient spectra and primary processes in the flash photolysis of CH3SSCH3, CH3SCH3, CH3SH and C2H5SH. *Transactions of the Faraday Society* **1970,** *66* (0), 1987-1995.
53. Bridges, L.; White, J. M., Photochemistry of methanethiol at 254 and 214 nm. *The Journal of Physical Chemistry* **1973,** *77* (2), 295-298.
54. Jensen, E.; Keller, J. S.; Waschewsky, G. C. G.; Stevens, J. E.; Graham, R. L.; Freed, K. F.; Butler, L. J., Dissociation dynamics of CH3SH at 222, 248, and 193 nm: An analog for probing nonadiabaticity in the transition state region of bimolecular reactions. *The Journal of Chemical Physics* **1993,** *98* (4), 2882-2890.
55. Skelton, J.; Adam, F. C., The Photolysis and Radiolysis of Simple Mercaptans in Dilute Glassy Matrices. *Canadian Journal of Chemistry* **1971,** *49* (21), 3536-3543.
56. Bridges, L.; Hemphill, G. L.; White, J. M., Photochemistry of ethanethiol at 254 and 214 nm. *The Journal of Physical Chemistry* **1972,** *76* (19), 2668-2673.
57. Steer, R. P.; Knight, A. R., Reactions of thiyl radicals. VI. Photolysis of ethanethiol.

Canadian Journal of Chemistry **1969,** *47* (8), 1335-1345.
58. Jacox, M. E.; Milligan, D. E., Matrix isolation study of the infrared spectrum of thioformaldehyde. *Journal of Molecular Spectroscopy* **1975,** *58* (1), 142-157.
59. Jacox, M. E.; Milligan, D. E., Matrix-Isolation Study of the Vacuum-Ultraviolet Photolysis of Methyl Fluoride. The Infrared Spectra of the Free Radicals CF, HCF, and H2CF. *The Journal of Chemical Physics* **1969,** *50* (8), 3252-3262.
60. Jacox, M. E.; Milligan, D. E., Matrix-Isolation Study of the Vacuum-Ultraviolet Photolysis of Methyl Chloride and Methylene Chloride. Infrared and Ultraviolet Spectra of the Free Radicals CCl, H2CCl, and CCl2. *The Journal of Chemical Physics* **1970,** *53* (7), 2688-2701.
61. Becke, A. D., Density-Functional Thermochemistry. III. The Role of Exact Exchange. *The Journal of Chemical Physics* **1993,** *98* (7), 5648-5652.
62. Lee, C.; Yang, W.; Parr, R. G., Development of the Colle-Salvetti correlation-energy formula into a functional of the electron density. *Physical Review B* **1988,** *37* (2), 785-789.
63. Cossi, M.; Rega, N.; Scalmani, G.; Barone, V., Energies, structures, and electronic properties of molecules in solution with the C-PCM solvation model. *Journal of Computational Chemistry* **2003,** *24* (6), 669-681.
64. Barone, V., Vibrational zero-point energies and thermodynamic functions beyond the harmonic approximation. *The Journal of Chemical Physics* **2004,** *120* (7), 3059-3065.
65. Barone, V., Anharmonic vibrational properties by a fully automated second-order perturbative approach. *The Journal of Chemical Physics* **2004,** *122* (1), 014108.
66. Bloino, J.; Barone, V., A second-order perturbation theory route to vibrational averages and transition properties of molecules: General formulation and application to infrared and vibrational circular dichroism spectroscopies. *The Journal of Chemical Physics* **2012,** *136* (12), 124108.
67. Bartlett, R. J.; Purvis, G. D., Many-body perturbation theory, coupled-pair many-electron theory, and the importance of quadruple excitations for the correlation problem. *International Journal of Quantum Chemistry* **1978,** *14* (5), 561-581.
68. Pople, J. A.; Krishnan, R.; Schlegel, H. B.; Binkley, J. S., Electron correlation theories and their application to the study of simple reaction potential surfaces. *International Journal of Quantum Chemistry* **1978,** *14* (5), 545-560.
69. Purvis, G. D.; Bartlett, R. J., A full coupled-cluster singles and doubles model: The inclusion of disconnected triples. *The Journal of Chemical Physics* **1982,** *76* (4), 1910-1918.
70. Scuseria, G. E.; Janssen, C. L.; Schaefer, H. F., An efficient reformulation of the closed-shell coupled cluster single and double excitation (CCSD) equations. *The Journal of Chemical Physics* **1988,** *89* (12), 7382-7387.
71. Pople, J. A.; Head-Gordon, M.; Raghavachari, K., Quadratic configuration interaction. A general technique for determining electron correlation energies. *The Journal of Chemical Physics* **1987,** *87* (10), 5968-5975.
72. Dunning, T. H., Gaussian Basis Sets for Use in Correlated Molecular Calculations. I. The Atoms Boron through Neon and Hydrogen. *The Journal of Chemical Physics* **1989,** *90* (2), 1007.
73. Kendall, R. A.; Dunning, T. H.; Harrison, R. J., Electron Affinities of the First-Row Atoms Revisited. Systematic Basis Sets and Wave Functions. *The Journal of Chemical Physics* **1992,** *96* (9), 6796.
74. Frisch, M. J.; Trucks, G. W.; Schlegel, H. B.; Scuseria, G. E.; Robb, M. A.; Cheeseman, J. R.; Scalmani, G.; Barone, V.; Mennucci, B.; Petersson, G. A.; Nakatsuji, H.; Caricato, M.; Li, X.; Hratchian, H. P.; Izmaylov, A. F.; Bloino, J.; Zheng, G.; Sonnenberg, J. L.; Hada, M.; Ehara, M.; Toyota, K.; Fukuda, R.; Hasegawa, J.; Ishida, M.; Nakajima, T.; Honda, Y.; Kitao, O.; Nakai, H.; Vreven, T.; Montgomery Jr., J. A.; Peralta, J. E.; Ogliaro, F.; Bearpark, M. J.; Heyd, J.; Brothers, E. N.; Kudin, K. N.; Staroverov, V. N.; Kobayashi, R.; Normand, J.; Raghavachari, K.; Rendell, A. P.; Burant, J. C.; Iyengar, S. S.; Tomasi, J.; Cossi, M.; Rega, N.; Millam, N. J.; Klene, M.; Knox, J. E.; Cross, J. B.; Bakken, V.; Adamo, C.; Jaramillo, J.; Gomperts, R.; Stratmann, R.

E.; Yazyev, O.; Austin, A. J.; Cammi, R.; Pomelli, C.; Ochterski, J. W.; Martin, R. L.; Morokuma, K.; Zakrzewski, V. G.; Voth, G. A.; Salvador, P.; Dannenberg, J. J.; Dapprich, S.; Daniels, A. D.; Farkas, Ã. d.; Foresman, J. B.; Ortiz, J. V.; Cioslowski, J.; Fox, D. J. *Gaussian 09*, Gaussian, Inc.: Wallingford, CT, USA, 2009.

75. Puzzarini, C.; Biczysko, M.; Barone, V., Accurate Harmonic/Anharmonic Vibrational Frequencies for Open-Shell Systems: Performances of the B3LYP/N07D Model for Semirigid Free Radicals Benchmarked by CCSD(T) Computations. *Journal of Chemical Theory and Computation* **2010,** *6* (3), 828-838.

76. Coupeaud, A.; Turowski, M.; Gronowski, M.; Piétri, N.; Couturier-Tamburelli, I.; Kołos, R.; Aycard, J.-P., C5N− anion and new carbenic isomers of cyanodiacetylene: A matrix isolation IR study. *The Journal of Chemical Physics* **2008,** *128* (15), 154303.

77. Kołos, R.; Gronowski, M.; Dobrowolski, J. C., Prospects for the Detection of Interstellar Cyanovinylidene. *The Astrophysical Journal* **2009,** *701* (1), 488.

78. Gronowski, M. Teoria I Eksperyment W Badaniach Spektroskopii Wybranych Nitryli O Znaczeniu Astrochemicznym Oraz Czasteczek Pokrewnych. PhD Thesis, Institute of Physical Chemistry Polish Academy of Sciences, Poland, Warszawa, 2010.

79. Szczepaniak, K.; Person, W. B., Measurement of the absolute infrared intensity of the fundamental vibration of HCl in low temperature matrices. *Journal of Molecular Structure* **1982,** *80*, 309-316.

80. Urso, R. G.; Scirè, C.; Baratta, G. A.; Compagnini, G.; Palumbo, M. E., Combined infrared and Raman study of solid CO. *Astronomy & Astrophysics* **2016,** *594*.

81. Seidel, G. M.; Lanou, R. E.; Yao, W. In *Rayleigh scattering in rare-gas liquids*, 2002.

82. Kisiel, Z.; Pszczolkowski, L., The Millimeter-Wave Rotational Spectrum of Chloroacetonitrile. *Journal of Molecular Spectroscopy* **1993,** *158* (2), 318-327.

83. Mollendal, H.; Samdal, S.; Guillemin, J. C., Rotational Spectrum, Conformational Composition, Intramolecular Hydrogen Bonding, and Quantum Chemical Calculations of Mercaptoacetonitrile (HSCH2CN), a Compound of Potential Astrochemical Interest. *J Phys Chem A* **2016,** *120* (12), 1992-2001.

84. Dobrowolski, J. C.; Jamróz, M. H.; Kołos, R.; Rode, J. E.; Cyrański, M. K.; Sadlej, J., IR low-temperature matrix, X-ray and ab initio study on l-isoserine conformations. *Physical Chemistry Chemical Physics* **2010,** *12* (36), 10818-10830.

85. Dobrowolski, J. C.; Jamróz, M. H.; Kołos, R.; Rode, J. E.; Sadlej, J., IR Low-Temperature Matrix and ab Initio Study on β-Alanine Conformers. *ChemPhysChem* **2008,** *9* (14), 2042-2051.

86. Turowski, M.; Gronowski, M.; Custer, T.; Zapala, J.; Guillemin, J. C.; Kołos, R., Isomerization of methyl isothiocyanate and methyl thiocyanate in argon matrices induced by UV irradiation. in preparation.

87. Dendramis, A.; Leroi, G. E., Matrix isolation spectroscopic study of the free radical HCCN. *The Journal of Chemical Physics* **1977,** *66* (10), 4334-4340.

88. Maier, G.; Reisenauer, H. P.; Rademacher, K., Cyanocarbene, Isocyanocarbene, and Azacyclopropenylidene: A Matrix-Spectroscopic Study. *Chemistry – A European Journal* **1998,** *4* (10), 1957-1963.

89. Cho, H.-G.; Andrews, L., Matrix Infrared Spectra and Density Functional Calculations of the H2CCN and H2CNC Radicals Produced from CH3CN. *The Journal of Physical Chemistry A* **2011,** *115* (31), 8638-8642.

90. Isoniemi, E.; Pettersson, M.; Khriachtchev, L.; Lundell, J.; Räsänen, M., Infrared Spectroscopy of H2S and SH in Rare-Gas Matrixes. *The Journal of Physical Chemistry A* **1999,** *103* (6), 679-685.

91. Koda, S.; Koga, K.; Takizawa, K.; Ihara, Y.; Takami, A., *Photodissociation of H 2S doped in low temperature rare gas solids under UV irradiation*. 2001; Vol. 274, p 283-289.

92. Continetti, R.; Balko, B.; Lee, Y. T., *Photodissociation of H2S and the HS radical at 193.3 nm*. 1991; Vol. 182, p 400-405.

93. Khriachtchev, L.; Pettersson, M.; Isoniemi, E.; Räsänen, M., 193 nm photolysis of H2S in rare-gas matrices: Luminescence spectroscopy of the products. *The Journal of Chemical Physics* **1998,** *108* (14), 5747-5754.
94. Szczepanski, J.; Hodyss, R.; Fuller, J.; Vala, M., Infrared Absorption Spectroscopy of Small Carbon−Sulfur Clusters Isolated in Solid Ar. *The Journal of Physical Chemistry A* **1999,** *103* (16), 2975-2981.
95. Pacansky, J.; Bargon, J., Low temperature photochemical studies on acetyl benzoyl peroxide. Observation of methyl and phenyl radicals by matrix isolation infrared spectroscopy. *Journal of the American Chemical Society* **1975,** *97* (23), 6896-6897.
96. Snelson, A., Infrared matrix isolation spectrum of the methyl radical produced by pyrolysis of methyl iodide and dimethyl mercury. *The Journal of Physical Chemistry* **1970,** *74* (3), 537-544.
97. Kappe, C. O.; Wah Wong, M.; Wentrup, C., Matrix isolation and infrared spectrum of thioformyl cyanide. *Tetrahedron Letters* **1993,** *34* (41), 6623-6626.
98. Kameneva, S. V.; Volosatova, A. D.; Feldman, V. I., Radiation-induced transformations of isolated CH3CN molecules in noble gas matrices. *Radiation Physics and Chemistry* **2017,** *141*, 363-368.
99. Wierzejewska, M.; Mielke, Z., Photolysis of isothiocyanic acid HNCS in low-temperature matrices. Infrared detection of HSCN and HSNC isomers. *Chemical Physics Letters* **2001,** *349* (3), 227-234.
100. Anderson, D. T.; Davis, S.; Nesbitt, D. J., Sequential solvation of HCl in argon: High resolution infrared spectroscopy of ArnHCl (n=1,2,3). *The Journal of Chemical Physics* **1997,** *107* (4), 1115-1127.
101. Kalinowski, J.; Gerber, R. B.; Räsänen, M.; Lignell, A.; Khriachtchev, L., Matrix effect on vibrational frequencies: Experiments and simulations for HCl and HNgCl (Ng = Kr and Xe). *The Journal of Chemical Physics* **2014,** *140* (9), 094303.
102. Lorenz, M.; Kraus, D.; Räsänen, M.; Bondybey, V. E., Photodissociation of hydrogen halides in rare gas matrices, and the effect of hydrogen bonding. *The Journal of Chemical Physics* **2000,** *112* (8), 3803-3811.
103. Howard, B. J.; Pine, A. S., Rotational predissociation and libration in the infrared spectrum of Ar□HCl. *Chemical Physics Letters* **1985,** *122* (1), 1-8.
104. Boulet, C.; Flaud, P. M.; Hartmann, J. M., Infrared line collisional parameters of HCl in argon, beyond the impact approximation: Measurements and classical path calculations. *The Journal of Chemical Physics* **2004,** *120* (23), 11053-11061.
105. Lee, Y. P.; Pimentel, G. C., Chemiluminescence of S2 in solid argon. *The Journal of Chemical Physics* **1979,** *70* (2), 692-698.
106. Brom, J. M.; Lepak, E. J., Afterglow from the photodissociation OCS in an argon matrix at 4K. *Chemical Physics Letters* **1976,** *41* (1), 185-187.

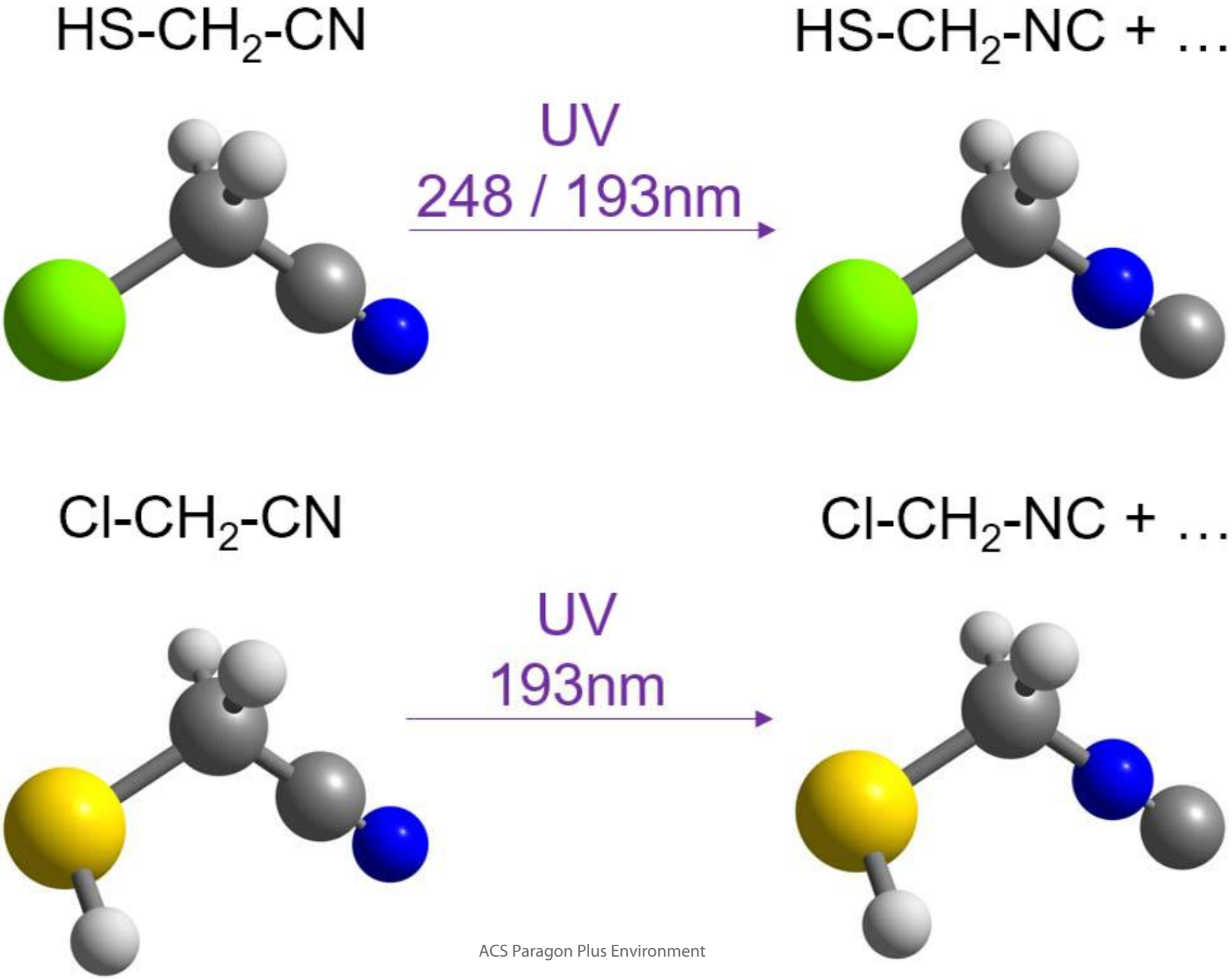
HS-CH2-CN
HS-CH2-NC + …
UV
248 / 193nm
Cl-CH2-CN
Cl-CH2-NC + …
UV
193nm